Mathematical Biosciences and Engineering

MBE, 22(12): 2988–3004.
DOI: 10.3934/mbe.2025110
Received: 7 May 2025
Revised: 10 July 2025
Accepted: 22 July 2025
Published: 24 September 2025

http://www.aimspress.com/journal/MBE

Research article

Working Set: adapted model to the epidemiological context

Aslanbek Murzakhmetov[1,2,*], Gaukhar Borankulova[1], Aigul Tungatarova[1], Saltanat Dulatbayeva[1], Nurgul Zhoranova[1] and Zhazira Taszhurekova[1]

[1] Department of Information Systems, Faculty of Technology, M.Kh. Dulaty Taraz University, Taraz 080001, Kazakhstan
[2] School of Information Sciences, University of Illinois Urbana-Champaign, IL 61801, USA

* **Correspondence:** Email: aslanbek@illinois.edu.

Abstract: The necessity of modeling the dynamics of infectious disease spread is driven by the imperative to accurately predict epidemics and assess the efficacy of control measures, such as isolation and quarantine. Conventional compartmental SIR and SEIR models have been widely used for predicting the course of epidemics, but they have limitations due to their inability to account for dynamic isolation. Research frequently recognizes the assumptions underlying these models but rarely provides justification for their validity within the specific contexts where they are applied. In this paper, we propose a novel approach based on the concept of a working set, which we utilize as a subset of agents actively involved in social contact and potential transmission. Our adapted working set model incorporates isolation states for susceptible and infected agents, enabling dynamic adjustment of the transmission rate according to the current size of the Working Set. The incorporation of a time window parameter enables the identification of current contacts and the identification of superspreaders, an important component for the optimization of epidemiological measures. Experimental results and comparative analysis showed that, compared to the SIR and SEIR models, the adapted working set model provides a more detailed and realistic tool for analyzing the spread of infection under dynamic control measures. Our model accounts for contact heterogeneity and allows a better assessment of the impact of isolation. The presented approach integrates resource management principles from computer systems with epidemiological models, providing a flexible and realistic tool for evaluating and optimizing infectious disease control measures. In addition, a practical analysis of established models reveals fundamental modeling principles that can be adapted to different scenarios.

Keywords: Working Set; compartmental models; complex systems; epidemic spreading; page replacement; page fault; computer simulations

1. Introduction

Compartmental models, such as susceptible-infected-recovered (SIR), susceptible–exposed–infected-recovered (SEIR), and SEIR-V, have been widely used to study infectious disease outbreaks [1]. These models are successive mathematical extensions, each adding new aspects to more accurately model and analyze the spread of infectious diseases. They divide populations into groups (compartments) based on disease status and use differential equations to describe the transitions between them. The SIR model proposed in Kermack and McKendrick [2] is a seminal work in the field of infectious disease modeling. In [2], Kermack and McKendrick introduced a foundational epidemiological model that segments the population into three compartments: susceptible (S), infected (I), and recovered (R). This model is widely known as the SIR model. Notably, as a special case of their general framework, the authors proposed a simple system of ordinary differential equations (ODEs) to describe the time evolution of population proportions in each compartment of the SIR model. However, the classical SIR model is not entirely realistic because it assumes that individuals immediately become infectious upon exposure, while most infectious or transmissible diseases have an incubation period. The incubation period can be incorporated into the SIR framework by adding an additional compartment, resulting in the SEIR system, which accounts for exposed or incubating individuals [3,4]. Although the SIR model is mathematically simpler and sometimes more convenient to analyze, it lacks epidemiological and biological realism [5,6]. An extended version of SEIR is the SEIR-V model, which adds the vaccinated category V to account for the effect of vaccination on the spread of infection [7,8]. For greater accuracy, compartmental models are often combined with agent-based models to account for individual differences in behavior and social networks [9−11]. However, the SIR, SEIR, and SEIR-V models have limitations, especially in the context of dynamic control measures such as isolation or quarantine. The main limitation of these models is that they assume all susceptible and infected agents interact freely with each other—that is, everyone has an equal chance of getting infected by anyone else [12,13]. This is known as the homogeneous mixing assumption. In reality, when measures like isolation of infected individuals are implemented, interactions between groups are significantly reduced, and such behavior cannot be adequately modeled by classical models without additional modifications.

Isolation and quarantine are important measures for preventing the spread of infection during epidemics, as shown in [14,15]. They are important tools during epidemics because they prevent the spread of disease, protect vulnerable groups, allow time for monitoring and treatment, reduce the burden on health systems, facilitate contact tracing, and have proven historical effectiveness. Despite the potential social and economic costs, their benefits in controlling epidemics are significant, making them an integral part of public health strategies. To analyze epidemic dynamics and to evaluate the effectiveness of control measures such as isolation, we propose an adapted working set (WS) model originally developed in computer science, namely in memory management systems. The adaptive WS model includes isolation as a central element, where agents can be removed from the working set, thereby reducing the transmission potential.

The working set model, proposed by Denning [16,17], describes the set of memory pages that are actively used by a process at a given time, and the unloading of infrequently used pages. It is used to

minimize page faults and improve system performance. The WS of a process is defined as the set of memory pages used during a given time interval. It is formally written as $W(t,\tau)$, where t is the current time, and τ is the length of the time window. If a page is used frequently during τ, it is not excluded from the working set. Our primary aim is to demonstrate the application of a working set model to an epidemiological context.

We define a working set as a subset of agents in contact with each other, among which there may be agents actively involved in contact transmission. In our adapted WS model, agents actively involved in transmission are excluded from the WS, i.e., are isolated from the group. Thus, the algorithm of the WS model is used as a way to identify superspreaders [18] that transmit the infection to a large number of susceptible agents through frequent contact, communication, or inter-agent contact. Unlike classical models such as SIR or SEIR, our adaptive WS model accounts for dynamic isolation and varying transmission rates depending on the size of the working set. Therefore, this paper proposes an adaptation of the WS model to an epidemiological context in order to model the dynamics of infectious disease spread under various control measures. While the WS model introduces dynamic isolation and adjusts transmission rates based on the size of the active working set, it still assumes a simplified contact structure. In contrast, network-based models explicitly represent contact heterogeneity through graph structures, where nodes represent individuals and edges represent interactions. Notable examples include the framework presented in [19, 20], which analyzes epidemic processes in complex networks, and the SEI model with backward bifurcations in heterogeneous populations. These models capture clustering, degree distributions, and community structures that influence epidemic thresholds and dynamics. Although our model does not explicitly construct a contact network, it approximates heterogeneity by dynamically adjusting the working set based on recent contact activity. Future work will explore hybrid approaches that integrate WS dynamics with network-based representations to better capture real-world contact structures.

2. Materials and methods

We first review the basic SIR model of Kermack and McKendrick, where the proportions of agents in susceptible, infected, and removed compartments satisfy the following system of ODEs:

$$\begin{cases} \dfrac{dS}{dt} = -\beta \dfrac{SI}{N} \\ \dfrac{dI}{dt} = \beta \dfrac{SI}{N} - \gamma I \\ \dfrac{dR}{dt} = \gamma I \end{cases} \tag{1}$$

where β is the disease transmission rate, representing the average number of contacts per agent per unit time multiplied by the probability of transmission; γ is the recovery rate, representing the average rate at which infected individuals recover; $N = S + I + R$ is the total population size N held constant in the base model.

The key parameter is the base reproductive rate R_0, calculated as $R_0 = \beta/\gamma$. Here, R_0 is the average number of secondary infections caused by an infected individual in a fully susceptible population. If $R_0 > 1$, the disease spreads; if $R_0 < 1$, it dies out.

SEIR (with incubation period):

$$\begin{cases} \dfrac{dS}{dt} = -\beta \dfrac{SI}{N} \\ \dfrac{dE}{dt} = \beta \dfrac{SI}{N} - \sigma E \\ \dfrac{dI}{dt} = \sigma E - \gamma I \\ \dfrac{dR}{dt} = \gamma I \end{cases} \tag{2}$$

where σ is the E to I transition coefficient, i.e., the rate at which exposed individuals become infectious ($1/\sigma$ is the average duration of the latency period); β and γ are similar to the SIR model.

2.1. Details of the model

We now examine some key assumptions of the WS model adapted to epidemiology. Key elements of the original WS model are redefined as follows: *Population*: The complete set of agents in a system, analogous to the set of all memory pages in a computer model. *Working set:* A subset of the population that includes agents that are not currently isolated and may be involved in transmission. *Isolation:* The process of excluding agents from the working set, equivalent to unloading pages from RAM. Isolated agents are temporarily not involved in the spread of infection. *Superspreader:* An infected agent (in state I) that transmits infection to an unusually large number of susceptible agents (state S). Unlike the average infected agent, a superspreader causes significantly more infections due to high contact frequency or other factors.

2.2. Definition of states in the model

The adapted model introduces the following states that reflect the epidemiologic status of the agents: *Susceptible* (S): agents that can become infected through contact with infected agents. *Infected* (I): agents capable of transmitting infection to others. *Recovered* (R): agents who have developed immunity and are no longer involved in transmission. *Isolated* (Z): these are infected agents or, in rare cases, susceptible agents that are physically separated from the rest to prevent further spread of the disease. The adaptive WS model is described by a system of ODEs:

$$\begin{cases} \dfrac{dS}{dt} = -\beta(t) \dfrac{SI}{N_{WS}} - \delta_S S + \eta_S Z_S \\ \dfrac{dI}{dt} = \beta(t) \dfrac{SI}{N_{WS}} - \gamma I - \delta_I I \\ \dfrac{dR}{dt} = \gamma I + \eta_I Z_R \\ \dfrac{dZ_S}{dt} = \delta_S S - \eta_S Z_S \\ \dfrac{dZ_R}{dt} = \gamma Z_I - \eta_I Z_R \end{cases} \tag{3}$$

where Z_S is the isolated susceptible; Z_I is the isolated infected; Z_R is the isolated recovered (transferred from Z_I after recovery); $\beta(t)$ is the dynamic infection rate; N_{WS} is the current working set size (sum of agents in states S and I) at time *t*; δ_S is the isolation rate for S; δ_I is the isolation rate for I; η_S is the isolation release rate for S; η_I is the isolation release rate for I; and γ is the rate of recovery.

This system accounts for all key processes: infection, recovery, isolation, and release. The total population in the model is defined as follows:

$$N = S(t) + I(t) + R(t) + Z_S(t) + Z_I(t) + Z_R(t) \tag{4}$$

The size of the working set is determined by the formula $N_{WS}(t) = S(t) + I(t)$.

2.3. Dynamics of transitions between states

The dynamics of infection spread in the model are determined by the following processes:

1) *Infection*: Transition of agents from state S to I by contact with infected agents. The speed of this process depends on the frequency of contact and the probability of transmission:

$$\beta(t) = \frac{S(t)I(t)}{N_{WS}(t)} \tag{5}$$

2) *Recovery*: Transition from I to R as infected agents recover. Rate of transition from I to R will be $\gamma I(t)$.

3) *Isolation:* The transfer of agents from I or S to Z as a result of control measures such as contact tracing or isolation. Then, the coefficient from I to Z_I will be $\delta_I I(t)$, and from S to Z_S will be $\delta_S S(t)$.

4) *Release from isolation:* Return of agents from Z_S to S (if they remain susceptible) or to R (if recovered) after completion of the isolation period or confirmation of status by calculating $\eta_S Z_S(t)$. From Z_I to Z_R (recovery in isolation): $\gamma Z_I(t)$. From Z_R to R: $\eta_I Z_R(t)$.

2.4. Impact on the rate of transmission of infection

In contrast to traditional models such as SIR, where the infection rate β is assumed to be constant and the population is assumed to be homogeneously mixed, in the adapted WS model, the value of β becomes a dynamic variable depending on the size of the working set:

$$\beta(t) = \beta_0 \times \frac{N_{WS}(t)}{N} \tag{6}$$

where β_0 is the basic transmission rate under full population conditions.

In computer systems, the working set defines a subset of active resources that minimizes delays. Similarly, in an epidemiological context, N_{WS} reflects a group of agents involved in the transmission of infection. The reduction of N_{WS} through isolation reduces the frequency of contacts, which is a key factor in β_t. The linear dependence here is the first approximation corresponding to the homogeneous mixing of the population. The linear approximation reflects the average reduction of contacts during isolation. As the number of isolated agents increases, the size of the WS decreases, which reduces $\beta(t)$ and slows the spread of infection. This approach allows us to model the effect of isolation and other control measures on epidemic dynamics.

Human populations are heterogeneous in many aspects: social connections among agents display clustered community patterns [21−23], susceptibility and infectiousness potential vary widely due to age, health, or behavioral differences, and geographic regions often implement distinct epidemic containment strategies. The long-standing assumption of uniform, well-mixed populations has been rigorously tested through heterogeneous modeling frameworks [24−28]. To summarize the effects of uneven transmission likelihoods, vulnerability distributions, and interaction patterns, we use a simple class of models in which the population is partitioned into multiple groups of agents [29−31]. These adaptations aim to demonstrate that population diversity can significantly alter both the progression and total reach of an epidemic and, critically, broaden the range of viable intervention strategies.

Let us consider a multi-agent system (MAS) with *n* agents distributed over *p* groups and exposed to the risk of infection through contact with each other. In our understanding, MAS consists of a finite number of agents and an environment that hosts agents in which agents act and react to other agents. Let us specify the agents' distribution into groups, and each agent group number can be easily determined by the Boolean matrix $x = (x_{ri})_{p\times n}$, where the element is $x_{ri} = 1$, if the agent with the number i is located in the group with the number *r* and $x_{ri} = 0$, otherwise. The matrix x must satisfy constraints (a), (b), and (c). Whatever the distribution of agents over groups, we assume that each agent of the system belongs to only one of the groups (condition, (a)):

$$\sum_{r=1}^{p} x_{ri} = 1, \qquad i = 1,2,\dots,n. \qquad (a)$$

Each agent of the system is assigned a weight, the linear size of its living space, within which the agent can perform its set of operations assigned to it. In this case, the agents interacting with each other are exposed to infection risk through contact. Each group is also assigned a weight, a living space within which the group's agents are located. The total weight of agents in any group should not exceed the weight of the group (condition (b)):

$$\sum_{i=1}^{n} l_i \cdot x_{ri} \le v_r, \qquad r = 1,2,\dots,p. \qquad (b)$$

Here, l_i is the weight of the agent i, $i = 1,2,\dots,n$, and v_r is the weight of the group with number *r*, *r*=1, 2, ... , *p*. Let us determine the number of a group that contains an agent, for example i, with a given matrix $x \in$ X, denoting this number by $r_i(x)$ and taking into account the constraints $(a), (b)$, and we write:

$$r_i(x) = \sum_{r=1}^{p} x_{ri} \cdot r, \qquad i = 1,2,\dots,n. \qquad (c)$$

3. Modeling and results

A WS in an epidemiological context is a dynamic group of agents that participate in social interactions and are not subject to isolation. Its size and composition depend on the following factors: *Isolation policy*: when an infected agent from I is identified, its contacts from S in the last τ days are relegated to the state Z. This shortens the WS and reduces the likelihood of new infections. At the end of the isolation period, agents from Z are tested: susceptible agents return to S, recovered agents to R. An alternative scenario is high-coverage isolation, in which a large fraction of the population is

isolated. *Time window* (τ): similar to the original WS model, a parameter τ is introduced to define the period of "relevance" of contacts. Agents who have been in contact with infected agents in the last τ time units are considered candidates for isolation. There may also be superspreaders among these agents. Their identification is important for epidemic control because the isolation of such agents can significantly slow the spread of the disease. In the WS model, the τ parameter specifies the time window during which contacts are considered relevant.

3.1. Numerical simulations

To assess the dynamics of infection spread and evaluate the impact of isolation measures, focusing on the isolation period and the effectiveness of the various scenarios, we created three different scenarios of isolation rates. 1) Basic scenario: no isolation ($\delta_S = 0,\ \delta_I = 0$); 2) moderate isolation: low isolation parameters ($\delta_S = 0.05,\ \delta_I = 0.1$); 3) high-coverage isolation: high isolation parameters ($\delta_S = 0.2,\ \delta_I = 0.3$). The SIR and SEIR models do not take insulation into account, so only the basic scenario is considered. Table 1 shows the values of parameters and descriptions used for numerical simulations. These parameters were generated from an extensive literature review [32−36] of COVID-19 and epidemic modeling. In contrast to agent-based models [37−40], which are tailored to specific countries or regions, our model is designed for a generalized small-city population. This abstraction enables flexible adaptation and does not require detailed prior knowledge of regional parameters.

Table 1. Model parameters and descriptions.

Variable	Default value	Explanation
N	10.000	Total number of agents in the population
S_0	9.970	Initial number of susceptible agents
I_0	30	Initial number of infected agents
R_0	0	Initial number of recovered agents
E_0	0	Initial number of exposed agents (for SEIR model)
Z_{S_0}	0	Initial number of isolated susceptible agents
Z_{I_0}	0	Initial number of isolated infected agents
β	0.3	Infection rate; probability of disease transmission per contact between susceptible and infected agents
β_0	0.3	Base infection rate for the working set
σ	0.2	Incubation rate; rate at which exposed agents become infectious (for SEIR model)
γ	0.1	Recovery rate; proportion of infected agents recovering per unit time
η_S	0.1	Isolation release rate for susceptible agents;
η_I	0.1	Isolation release rate for infected agents.

We used an agent-based model that allows us to model different strategies in a virtual population and compare these strategies to get an idea of their optimal parameters. This approach is particularly advantageous because agent-based models capture the heterogeneity of individual agents and their interactions, which are often oversimplified or neglected in classical analytical methods. Unlike aggregate mathematical models, they enable the simulation of emergent behaviors that arise from local rules and micro-level dynamics. Such models also provide flexibility in testing a wide range of scenarios and policy interventions under varying assumptions [41,42]. As shown in Figure 1, we

performed a sensitivity analysis to evaluate the WS model's robustness to changes in key parameters. We varied β from 0.2 to 0.5, γ from 0.05 to 0.15, and δ_S and δ_I from 0.0 to 0.3.

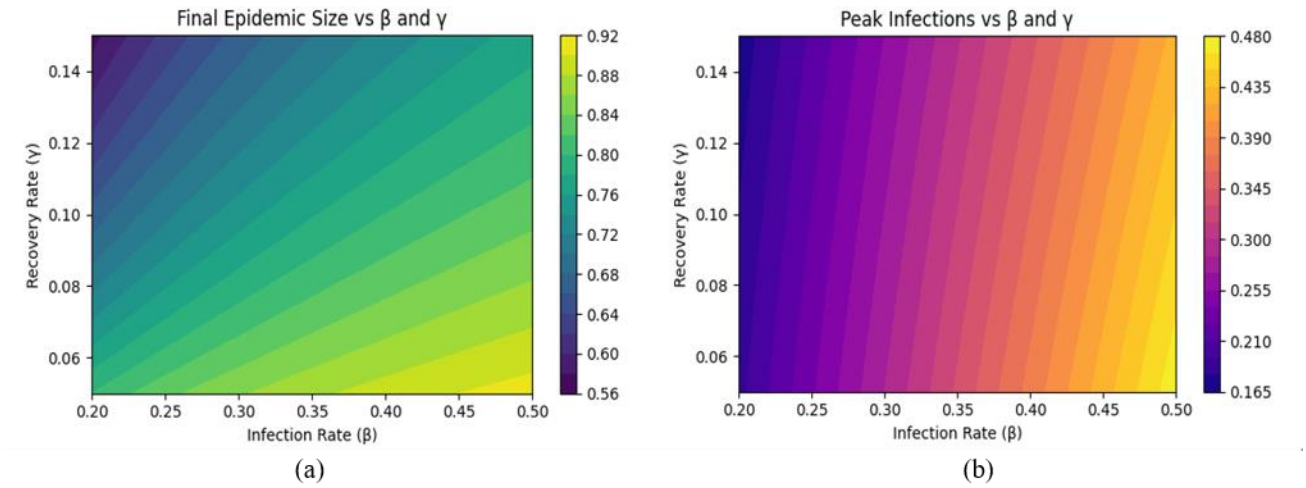

Figure 1. Sensitivity analysis of WS model: a) Final epidemic size as a function of β and γ. Epidemic coverage is highest when β is high and γ is low. b) Peak number of infections also occurs at high β and low γ. This is important for assessing the burden on the healthcare system and resource planning.

By modeling the spread of an infection, we are able to trace a typical epidemiological dynamic that progresses through several key stages. Figure 2 illustrates the dynamics of the epidemic spread process, including spatial distribution, formation of infection clusters, the role of superspreaders, and the impact of isolation measures on the spread of infection. As illustrated in Figure 2(a), the initial stage of the epidemic is characterized by a population consisting predominantly of susceptible agents, with an infection rate that is just beginning to manifest due to a limited number (0.3%) of infected agents. As shown in Figure 2(b), as the epidemic progresses, the proportion of infected agents increases to 2.4%, the first isolated agents appear, the amount of which is 0.08%, and superspreaders emerge at 0.18% in 10 days. These superspreaders play a critical role by rapidly infecting the surrounding community and forming the first foci of infection; in this case, clusters of agents. In the early stages of an outbreak, local foci of infection emerge around each superspreader, as illustrated by the red circles. We define a superspreader as an infected agent who has had contact with more than θ agents within the time window τ. In our simulations, we set $\theta = 20$, based on the upper 5% quantile of the contact distribution observed in the basic scenario. As illustrated in Figure 2(c), the proportion of infected agents increases to 18%, the number of isolated agents rises to 11%, and the proportion of superspreaders increases to 13%. As the epidemic progresses, small foci coalesce into a "cluster network", and transmission "bridges" between groups of agents emerge, thereby accelerating the spread of the infection. As illustrated in Figure 2(d), the initial recovered agents that were released following the isolation period are represented by the gray squares. The number of susceptible agents experiences a substantial decrease. At the peak of the epidemic, as shown in Figure 2(e), the proportion of susceptible agents constitutes –0.2% of the total population. The proportion of infected agents reaches –12%, the superspreaders –51%, isolated agents –26%, and recovered agents –10.8% on day 59.

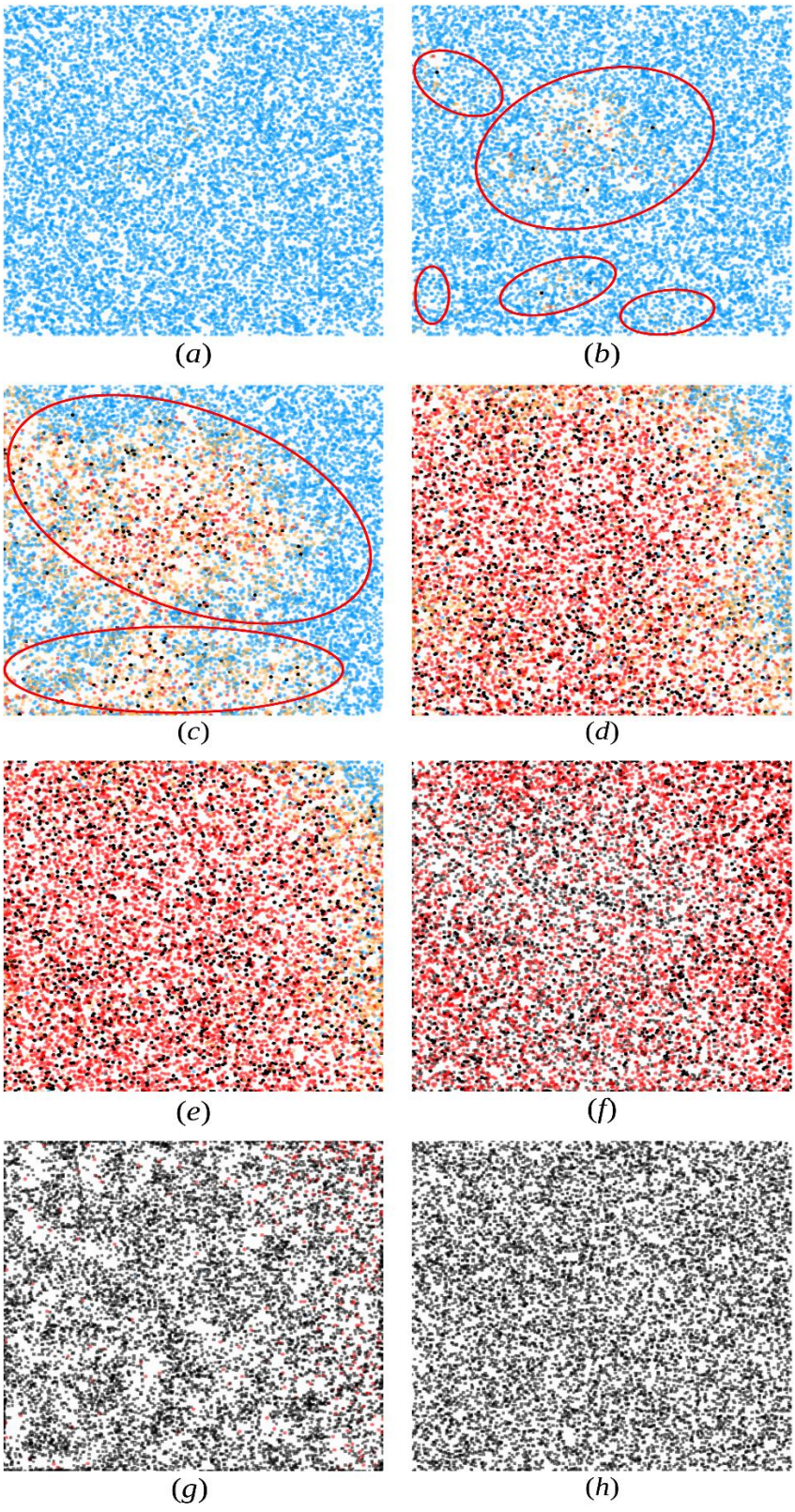

Figure 2. Epidemic dynamics in an agent-based population for 100 days, considering five types of agents with a total population of 10,000 agents: blue, susceptible agents; orange, infected agents; red, superspreaders; black, isolated agents; gray, recovered agents.

The implementation of more stringent isolation protocols at this point emerges as a pivotal factor in the mitigation of the propagation of infection. The proportion of isolated agents stands at 38%, thereby impeding further dissemination of the infection. In Figure 2(g), the proportion of infected agents is approximately 5%, superspreaders account for 41%, and isolated individuals comprise about 21%. The proportion of recovered agents is 32%. As illustrated in Figure 2(h), the final stage of the infection virtually disappears, and all agents are recovered within 100 days. The simulations underscore the pivotal function of superspreaders in expediting the propagation of the epidemic and the paramount importance of prompt isolation measures in its control, a phenomenon that is vividly illustrated by the dynamics depicted in the figures.

Figure 3(a) shows a comparison of the dynamics of infected agents in the basic scenario for SIR, SEIR, and working set (without isolation). The SIR model shows a rapid increase in infections with a peak of 3049 on day 26, followed by a sharp decline. SIR shows the fastest and most intense epidemic due to the lack of delay in infection. In the SEIR model, the peak is lower at around 2000, and later, around day 51, due to the incubation period. SEIR slows the spread by exposing, lowering, and delaying the peak. The WS model results are consistent with SIR because there is no isolation. This confirms the correctness of the WS implementation in the absence of isolation, on par with SIR.

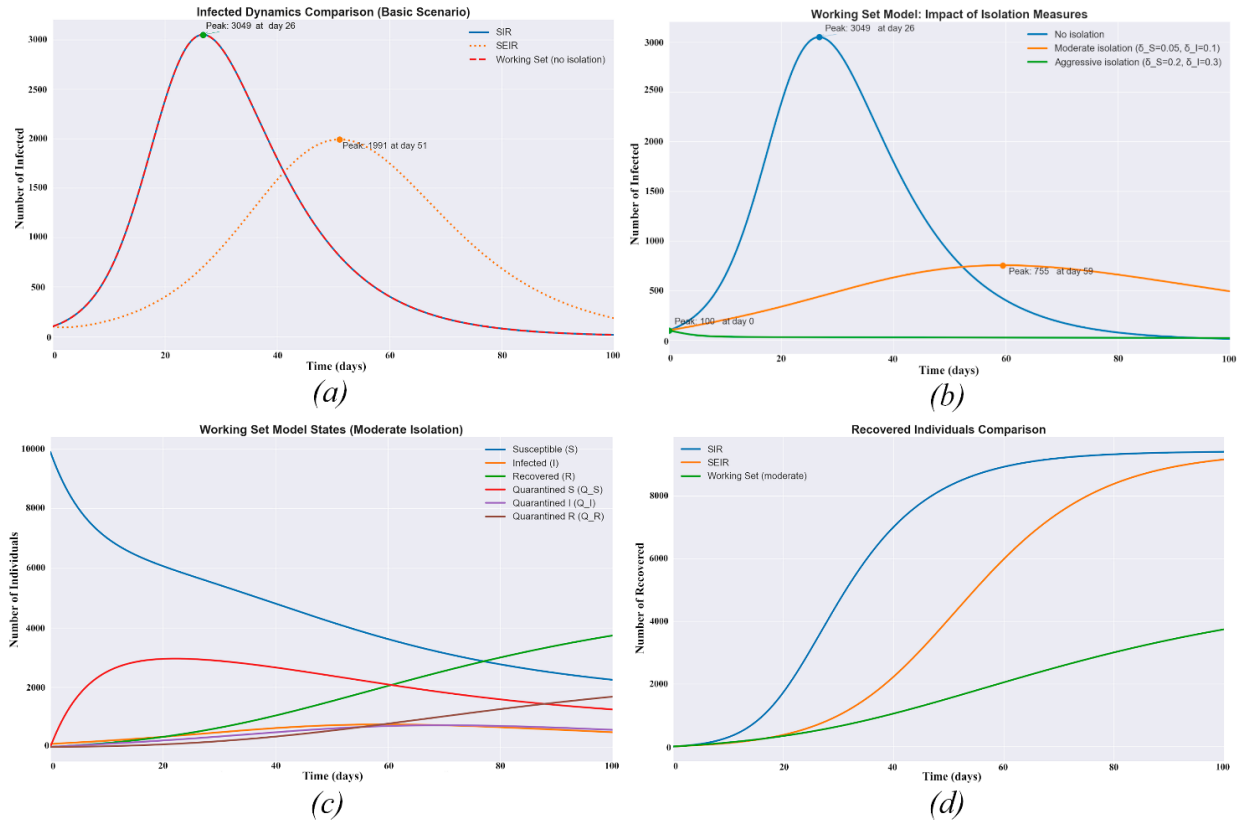

Figure 3. Comparative dynamics of epidemic progression in SIR, SEIR, and WS models: effects of incubation and isolation on infection peaks and epidemic size. (a) Comparison of infected agent dynamics in the basic scenario without isolation for the SIR, SEIR, and WS models. (b) Infection curves under three WS scenarios. (c) Evolution of all epidemiological states in the WS model under moderate isolation. (d) Comparison of the final number of recovered agents (R) across the models.

Figure 3(b) shows the dynamics of infected agents in the WS model for the three isolation scenarios. Without isolation, the peak of infected agents is 3050 on day 26. With moderate isolation, the peak drops to 755 and shifts to day 59. With high-coverage isolation, the peak shows 100 at the beginning, and then gradually decreases. The results show that isolation effectively "flattens the curve", reducing the peak of infection and slowing the epidemic. The high-coverage isolation with parameters $\delta_S = 0.2,\ \delta_I = 0.3$ is most effective, reducing the peak by a factor of three and allowing more time for preparation. Figure 3(c) shows the evolution of all states of the WS model with moderate isolation. The value of S decreases more slowly than in SIR due to the isolation. The peak of infected agents is about 2400 on day 20 and then declines steadily. This means that detection and isolation of superspreaders play a key role in controlling peak infections. As shown in Figure 3(d), the number of recovered (R) for the WS is much lower than SIR and SEIR. This is because the number of infected was lower due to isolation, and consequently, the number of cured is also lower. Isolation in the WS reduces the final size of the epidemic by preventing part of the population from being infected, while the SIR and SEIR models show larger epidemics due to the lack of isolation.

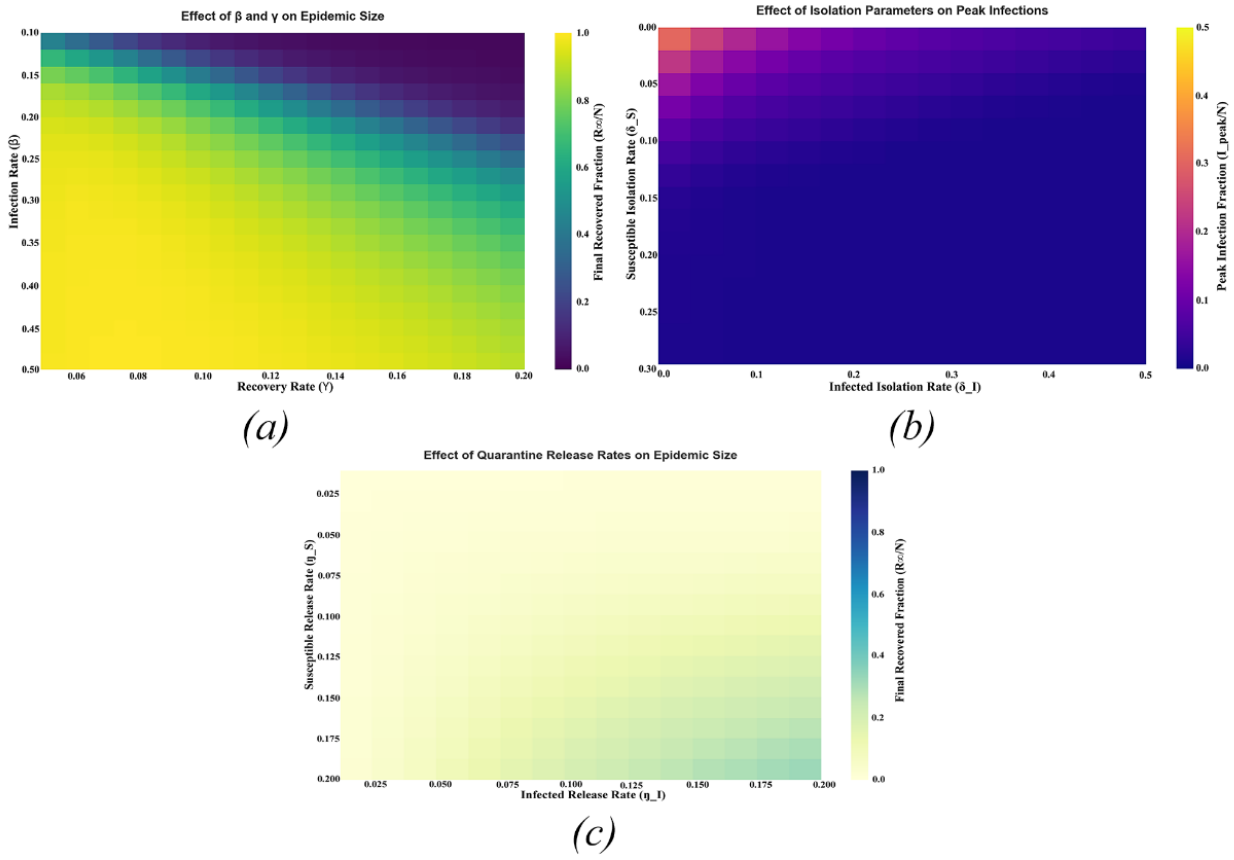

Figure 4. Sensitivity analysis of the working set model: heatmaps of epidemic outcomes under varying infection, recovery, and isolation parameters.

In Figure 4, epidemic sensitivity heatmaps of the working set model are shown. Figure 4(a) shows the final recovery rate as a function of the infection rate and recovery rate parameters; Figure 4(b) shows the analysis of the parameters of isolation of infected people, which is more effective in reducing the peak. But at the same time, strong isolation can significantly reduce the burden on the health system [43−46] or economy [47]. Figure 4(c) shows the rate of isolation release for the WS. A fast release from isolation

increases the size of the epidemic as people return to the active population. A slow release keeps the epidemic under control but requires more resources.

To evaluate the efficiency of the adapted WS model, we compare it with the classical SIR and SEIR models. Comparing the SIR, SEIR, and WS models, we can say that WS is flexible due to isolation, which makes it more realistic for modeling control measures.

Table 2. Comparison results of models.

Aspect	SIR/SEIR	Adapted WS
Isolation	Not directly accounted, expansion required	Included as centerpiece, dynamic adjustment
Transmission rate	Fixed or dependent on S and I	Dynamically adjusted based on active set
Contact heterogeneity	Requires extensions (e.g., network)	Modeled through agent grouping and dynamic subsets
Behavioral solutions	Not modeled	May be enabled via agent rules
Superspreader identification	Not explicitly modeled	Identified based on contact frequency within a time window
Intervention applicability	Limited without modifications	Easy to model isolation
Scalability	High (ODE-based), but limited realism	Moderate: more resource-intensive, but scalable via aggregation
Data requirements	Low: only aggregate parameters needed	Medium: requires contact data or distribution assumptions
Implementation simplicity	Simple to implement using differential equations	Moderate complexity, especially in agent-based implementations
Adaptability	Low without structural changes	High: easily adaptable to various scenarios and control strategies

The proposed adapted WS model has several advantages, like accounting for contact heterogeneity and the ability to quantify the impact of isolation, contact tracing, and other strategies. Also, similar to memory management in computer science, the model allows us to explore the effectiveness of epidemic control. These analyses demonstrate how an adapted WS model can be useful in investigating epidemic dynamics, providing valuable insights for infectious disease management. Further investigation of the model might be useful for health planning and evaluating measures such as isolation and social distancing.

4. Discussion

Although this paper primarily compares the classical SIR and SEIR models, it is important to note that several modern models also consider isolation and quarantine. For example, K-SEIR-Sim is a software based on a modified SEIR model that allows users to model the spread of infections while accounting for isolation, quarantine, and other containment measures. However, unlike the WS model, K-SEIR-Sim uses fixed parameters and does not dynamically update the agent workgroup based on current contacts. In contrast, the WS model allows for the adaptive exclusion of agents from active interactions, making it more flexible in the face of changing containment strategies. Additionally, there are network models, such as SIQR and extended graph-based SIR models, which allow us to consider the structure of social contacts

and introduce isolation at the level of network nodes. These models are well-suited for analyzing local outbreaks and optimizing quarantine measures. However, they require accurate network structure information and are often difficult to calibrate. In the future, it is planned to expand the scope of the current study to include a comparative analysis of the working set model with other state-of-the-art models supporting isolation mechanisms. In particular, approaches such as the K-SEIR-Sim software platform, which implements advanced quarantine scenarios, and network models of infection spread, which take into account the structure of social contacts and local containment measures, are of interest. A comparison with these models will allow for a more objective assessment of the advantages and limitations of the WS-model in the context of dynamic isolation and adaptive epidemic management. Consequently, such research will contribute to the further development of flexible and realistic tools for epidemiological modeling and response planning.

Agent-based implementation of the WS-model requires tracking contacts and states of a large number of agents. This can be resource intensive when modeling populations of tens or hundreds of thousands of people. However, unlike network models, WS does not require explicitly constructing a contact graph, which reduces memory and runtime requirements. Also, the model can be customized to fit the available resources. For example, aggregated workgroups can be used instead of individual agents, which allows the WS approach to be applied even in systems with limited computing power.

5. Conclusions

Epidemic modeling is a useful tool for understanding and controlling the spread of infectious diseases. The proposed working set model, adapted to the epidemiological context, offers a new approach to modeling the spread of infectious diseases and shows potential to improve the realism and responsiveness of epidemiological modeling, especially in the context of dynamic control measures such as isolation and quarantine. Unlike classical SIR and SEIR models, our model allows us to identify an active subset of agents as a "working set" that are directly involved in the transmission of infection. This approach allows us to account for heterogeneity in social contacts and to identify superspreaders, which is important for slowing epidemic growth. The introduction of dynamic isolation mechanisms allows more accurate modeling of the impact of control measures on the rate of disease spread. Despite some advantages, the WS model has certain limitations, including the complexity of the mathematical apparatus, the need for accurate empirical data, and detailed parameter calibration. Nevertheless, this approach, which combines resource management principles from computer science with epidemiological problems, offers prospects for the development of optimal epidemic control strategies.

Thus, the adapted working set model is a promising tool for analyzing and managing the spread of infectious diseases. Its use can facilitate a more accurate assessment of the impact of control measures, the development of optimal isolation strategies, and a timely response to epidemic threats. This study could help in the modeling of other similar diseases. Further research in this area will improve the model and integrate it with other approaches to improve public health planning in a rapidly changing epidemiological environment.

Use of AI tools declaration

The authors declare they have not used Artificial Intelligence (AI) tools in the creation of this article.

Acknowledgments

This research was funded by a grant from the Science Committee of the Ministry of Science and Higher Education of the Republic of Kazakhstan, grant number "AP19174930–Research and development of model for programs reorganization and data in segment-page systems based on two-level dictionary and geometric interpretation".

Conflict of interest

The authors declare there is no conflict of interest.

References

1. A. F. Siegenfeld, P. K. Kollepara, Y. Bar-Yam, Modeling complex systems: A case study of compartmental models in epidemiology, *Complexity*, **2022** (2022), 3007864. https://doi.org/10.1155/2022/3007864
2. W. O. Kermack, A. G. McKendrick, A contribution to the mathematical theory of epidemics, *Proc. R. Soc. A*, **115** (1927), 700–721. https://doi.org/10.1098/rspa.1927.0118
3. W. R. Khuda Bukhsh, G. A. Rempała, How to correctly fit an SIR model to data from an SEIR model?, *Math. Biosci*., **375** (2024), 109265. https://doi.org/10.1016/j.mbs.2024.109265
4. A. Korobeinikov, Global properties of SIR and SEIR epidemic models with multiple parallel infectious stages, *Bull. Math. Bio*., **71** (2009), 75–83. https://doi.org/10.1007/s11538-008-9352-z
5. E. Lara-Tuprio, C. S. Estadilla, T. Y. Teng, J. Uyheng, M. E. Estuar, E. K. E. Espina, et. al., Mathematical analysis of a COVID-19 compartmental model with interventions, in *Proceedings of the International Conference on Mathematical Sciences and Technology*, **2423** (2021), 020025. https://doi.org/10.1063/5.0075333
6. A. B. Gumel, E. A. Iboi, C. N. Ngonghala, E. H. Elbasha, A primer on using mathematics to understand COVID-19 dynamics: Modeling, analysis and simulations, *Infect. Dis. Modell*., **6** (2021), 148–168. https://doi.org/10.1016/j.idm.2020.11.005
7. J. A. Marques, F. N. Gois, J. Xavier-Neto, S. J. Fong, Epidemiology compartmental models—SIR, SEIR, and SEIR with intervention, in *Predictive Models for Decision Support in the COVID-19 Crisis*, Springer, (2021), 15–39. https://doi.org/10.1007/978-3-030-61913-8_2
8. A. Safarishahrbijari, T. Lawrence, R. Lomotey, J. Liu, C. Waldner, N. Osgood, Particle filtering in a SEIRV simulation model of H1N1 influenza, in *Proceedings of the Winter Simulation Conference*, (2015), 1240–1251. https://doi.org/10.1109/WSC.2015.7408249
9. X. Meng, Z. Cai, S. Si, D. Duan, Analysis of epidemic vaccination strategies on heterogeneous networks: Based on SEIRV model and evolutionary game, *Appl. Math. Comput*., **403** (2021), 126172. https://doi.org/10.1016/j.amc.2021.126172
10. K. R. Bissett, J. Cadena, M. Khan, C. J. Kuhlman, Agent-based computational epidemiological modeling, *J. Indian Inst. Sci.*, **101** (2021), 303–327. https://doi.org/10.1007/s41745-021-00260-2
11. F. A. Salem, U. F. Moreno, A multi-agent-based simulation model for the spreading of diseases through social interactions during pandemics, *J. Control Autom. Electr. Syst*., **33** (2022), 1161–1176. https://doi.org/10.1007/s40313-022-00920-3

12. O. Givan, N. Schwartz, A. Cygelberg, L. Stone, Predicting epidemic thresholds on complex networks: Limitations of mean-field approaches, *J. Theor. Biol*., **288** (2011), 21–28. https://doi.org/10.1016/j.jtbi.2011.07.015
13. M. Roberts, V. Andreasen, A. Lloyd, L. Pellis, Nine challenges for deterministic epidemic models, *Epidemics*, **10** (2015), 49–53. https://doi.org/10.1016/j.epidem.2014.09.006
14. A. Džiugys, M. Bieliūnas, G. Skarbalius, E. Misiulis, R. Navakas, Simplified model of Covid-19 epidemic prognosis under quarantine and estimation of quarantine effectiveness, *Chaos Solitons Fractals*, **140** (2020), 110162. https://doi.org/10.1016/j.chaos.2020.110162
15. A. James, M. J. Plank, S. Hendy, R. Binny, A. Lustig, N. Steyn, et al., Successful contact tracing systems for COVID-19 rely on effective quarantine and isolation, *PLoS One*, **16** (2021), e0252499. https://doi.org/10.1371/journal.pone.0252499
16. P. J. Denning, The working set model for program behavior, in *Proceedings of the ACM symposium on Operating System Principles*, (1967), 1–12. https://doi.org/10.1145/800001.811670
17. P. J. Denning, Working set analytics, *ACM Comput. Surv*., **53** (2021), 1–36. https://doi.org/10.1145/3399709
18. J. O. Lloyd-Smith, S. J. Schreiber, P. E. Kopp, W. M. Getz, Superspreading and the effect of individual variation on disease emergence, *Nature*, **438** (2005), 355–359. https://doi.org/10.1038/nature04153
19. W. Li, Y. Wang, J. Cao, M. Abdel-Aty, Dynamics and backward bifurcations of SEI tuberculosis models in homogeneous and heterogeneous populations, *J. Math. Anal. Appl*., **543** (2025), 128924, https://doi.org/10.1016/j.jmaa.2024.128924
20. R. Pastor-Satorras, C. Castellano, P. Van Mieghem, A. Vespignani, Epidemic processes in complex networks, *Rev. Mod. Phys*., **87** (2015), 925–979. https://doi.org/10.1103/RevModPhys.87.925
21. M. Girvan, M. E. J. Newman, Community structure in social and biological networks, *Proc. Natl. Acad. Sci*., **99** (2002), 7821–7826. https://doi.org/10.1073/pnas.122653799
22. A. Arenas, L. Danon, A. Diaz-Guilera, P. M. Gleiser, R. Guimer, Community analysis in social networks, *Eur. Phys. J. B*, **38** (2004), 373–380. https://doi.org/10.1140/epjb/e2004-00130-1
23. L. Hedayatifar, R. A. Rigg, Y. Bar-Yam, A. J. Morales, US social fragmentation at multiple scales, *J. R. Soc. Interface*, **16** (2019), 20190509. https://doi.org/10.1098/rsif.2019.0509
24. T. Britton, F. Ball, P. Trapman, A mathematical model reveals the influence of population heterogeneity on herd immunity to SARS-CoV-2, *Science*, **369** (2020), 846–849. https://doi.org/10.1126/science.abc6810
25. W. Gou, Z. Jin, How heterogeneous susceptibility and recovery rates affect the spread of epidemics on networks, *Infect. Dis. Modell*., **2** (2017), 353–367. https://doi.org/10.1016/j.idm.2017.07.001
26. R. I. Hickson, M. G. Roberts, How population heterogeneity in susceptibility and infectivity influences epidemic dynamics, *J. Theor. Biol*., **350** (2014), 70–80. https://doi.org/10.1016/j.jtbi.2014.01.014
27. A. Gerasimov, G. Lebedev, M. Lebedev, I. Semenycheva, COVID-19 dynamics: A heterogeneous model, *Front. Publ. Health*, **8** (2021), 558368. https://doi.org/10.3389/fpubh.2020.558368

28. J. Dolbeault, G. Turinici, Social heterogeneity and the COVID-19 lockdown in a multi-group SEIR model, *Comput. Math. Biophys*., **9** (2021), 14–21. https://doi.org/10.1515/cmb-2020-0115
29. P. Van Den Driessche, J. Watmough, Reproduction numbers and sub-threshold endemic equilibria for compartmental models of disease transmission, *Math. Biosci*., **180** (2002), 29–48. https://doi.org/10.1016/S0025-5564(02)00108-6
30. L. Hébert-Dufresne, B. M. Althouse, S. V. Scarpino, A. Allard, Beyond R_0: Heterogeneity in secondary infections and probabilistic epidemic forecasting, *J. R. Soc. Interface*, **17** (2020), 20200393. https://doi.org/10.1098/rsif.2020.0393
31. O. Diekmann, J. A. P. Heesterbeek, J. A. J. Metz, On the definition and the computation of the basic reproduction ratio R_0 in models for infectious diseases in heterogeneous populations, *J. Math. Biol*., **28** (1990), 365–382. https://doi.org/10.1007/BF00178324
32. S. I. Kabanikhin, O. I. Krivorotko, Mathematical modeling of the Wuhan COVID-2019 epidemic and inverse problems, *Comput. Math. and Math. Phys*., **60** (2020), 1889–1899. https://doi.org/10.1134/S0965542520110068
33. B. Lieberthal, A. M. Gardner, Connectivity, reproduction number, and mobility interact to determine communities' epidemiological superspreader potential in a metapopulation network, *PLoS Comput. Biol*., **17** (2021), e1008674. https://doi.org/10.1371/journal.pcbi.1008674
34. J. Chen, Y. Zhang, Y. Xu, C. Xia, J. Tanimoto, An epidemic spread model with nonlinear recovery rates on meta-population networks, *Nonlinear Dyn.*, **113** (2025), 3943–3957. https://doi.org/10.1007/s11071-024-10388-2
35. M. Horii, A. Gould, Z. Yun, J. Ray, C. Safta, T. Zohdi, Calibration verification for stochastic agent-based disease spread models, *PLoS One*, **19** (2024), e0315429. https://doi.org/10.1371/journal.pone.0315429
36. E. Taghizadeh, A. Mohammad-Djafari, SEIR modeling, simulation, parameter estimation, and their application for COVID-19 epidemic prediction, *Phys. Sci. Forum*, **5** (2022), 18. https://doi.org/10.3390/psf2022005018
37. K. Chen, X. Jiang, Y. Li, R. Zhou, A stochastic agent-based model to evaluate COVID-19 transmission influenced by human mobility, *Nonlinear Dyn*, **111** (2023), 12639–12655. https://doi.org/10.1007/s11071-023-08489-5
38. Q. Fan, Q. Li, Y. Chen, J. Tang, Modeling COVID-19 spread using multi-agent simulation with small-world network approach, *BMC Public Health*, **24** (2024), 672. https://doi.org/10.1186/s12889-024-18157-x
39. A. D. Wood, K. Berry, COVID-19 transmission in a resource dependent community with heterogeneous populations: An agent-based modeling approach, *Econom. Hum. Biol.*, **52** (2024), 101314. https://doi.org/10.1016/j.ehb.2023.101314
40. K. Gallagher, I. Bouros, N. Fan, E. Hayman, L. Heirene, P. Lamirande, et al., Epidemiological agent-based modelling software (Epiabm), *J. Open Res. Soft*., **12** (2024), 3. https://doi.org/10.5334/jors.449
41. A. Topîrceanu, On the impact of quarantine policies and recurrence rate in epidemic spreading using a spatial agent-based model, *Mathematics*, **11** (2023), 1336. https://doi.org/10.3390/math11061336

42. Y. Tatsukawa, M. R. Arefin, K. Kuga, J. Tanimoto, An agent-based nested model integrating within-host and between-host mechanisms to predict an epidemic, *PLoS One*, **18** (2023), e0295954. https://doi.org/10.1371/journal.pone.0295954
43. C. Nitzsche, S. Simm, Agent-based modeling to estimate the impact of lockdown scenarios and events on a pandemic exemplified on SARS-CoV-2, *Sci. Rep*., **14** (2024), 13391. https://doi.org/10.1038/s41598-024-63795-1
44. P. J. Schluter, M. Genereux, E. Landaverde, E. Y. Chan, K. C. Hung, R. Law, et al., An eight-country cross-sectional study of the psychosocial effects of COVID-19 induced quarantine and/or isolation during the pandemic, *Sci. Rep*., **12** (2022), 13175. https://doi.org/10.1038/s41598-022-16254-8
45. Y. Lin, L. Wu, H. Ouyang, J. Zhan, J. Wang, W. Liu, et al., Behavioral intentions and perceived stress under isolated environment, *Brain Behav*., **14** (2024), e3347. https://doi.org/10.1002/brb3.3347
46. U. Panchal, G. Pablo, M. Franco, C. Moreno, M. Parellada, C. Arango, et al., The impact of COVID-19 lockdown on child and adolescent mental health: systematic review, *Eur. Child Adolesc. Psychiatry*, **32** (2023), 1151–1177. https://doi.org/10.1007/s00787-021-01856-w
47. W. Yamaka, S. Lomwanawong, D. Magel, P. Maneejuk, Analysis of the lockdown effects on the economy, environment, and COVID-19 spread: Lesson learnt from a global pandemic in 2020, *Int. J. Environ. Res. Public. Health*, **19** (2022), 12868. https://doi.org/10.3390/ijerph191912868

AIMS Press